

# OVERVIEW OF RECENT MEASUREMENTS OF CP VIOLATION WITH $B$ MESONS AT LHCb\*

ROSE KOOPMAN

on behalf of the LHCb Collaboration

Nikhef, Amsterdam, The Netherlands

(Received April 14, 2014)

CP violation describes differences between matter and anti-matter. It is one of the three requirements to produce a matter dominated universe. We are now entering a new era with unprecedented data samples provided by the LHC, which allow to study flavour physics with high precision. LHCb has produced many first and world's best CP asymmetry measurements, in many different  $B$  meson decay modes, which provide a test of the Standard Model. This report presents an overview of recent measurements of CP violation in the  $B_{(s)}^0$  system, using the  $1 \text{ fb}^{-1}$  dataset collected with the LHCb detector.

DOI:10.5506/APhysPolB.45.1447

PACS numbers: 12.15.Hh, 13.25.Hw, 14.40.Nd

## 1. Introduction

One of the big scientific questions to date is why we live in a matter dominated universe. Charge-Parity (CP) violation is caused by differences between matter and anti-matter. It is one of the conditions postulated by Sakharov in 1967 needed in order to produce matter and anti-matter at different rates [1]. In 1964 CP violation was first discovered in  $K_L$  decays by Cronin and Fitch [2].

In the Standard Model (SM), CP violation is introduced via the Yukawa couplings which describe the interactions of the quarks to the Higgs field. Only the weak interactions violate CP. The flavour changing weak interactions are characterised by the Cabibbo–Kobayashi–Maskawa (CKM) matrix [3]

$$V_{\text{CKM}} = \begin{pmatrix} V_{ud} & V_{us} & V_{ub} \\ V_{cd} & V_{cs} & V_{cb} \\ V_{td} & V_{ts} & V_{tb} \end{pmatrix} \approx \begin{pmatrix} 1 - \frac{1}{2}\lambda^2 & \lambda & A\lambda^3(\rho - i\eta) \\ -\lambda & 1 - \frac{1}{2}\lambda^2 & A\lambda^2 \\ A\lambda^3(1 - \rho - i\eta) & -A\lambda^2 & 1 \end{pmatrix} \quad (1)$$

---

\* Presented at the Cracow Epiphany Conference on the Physics at the LHC, Kraków, Poland, January 8–10, 2014.

which is given here in the Wolfenstein parametrisation [4] to  $\mathcal{O}(\lambda^4)$ . The CKM matrix is a unitary matrix that carries four free parameters, three of which are real parameters and one is a complex phase. It is this complex phase,  $\eta$ , that allows for CP violation in the SM. Six orthogonality relations can be written down for the CKM matrix, which can be represented as triangles in the complex plane. The two triangles relevant to these proceedings are the triangle in the  $B^0$ -system described by  $V_{ud}V_{ub}^* + V_{cd}V_{cb}^* + V_{td}V_{tb}^* = 0$ , and the triangle in the  $B_s^0$ -system described by  $V_{us}V_{ub}^* + V_{cs}V_{cb}^* + V_{ts}V_{tb}^* = 0$ . The former is also referred to as the *unitarity triangle*. Figure 1 shows our current knowledge on the CKM matrix. Testing the unitarity of the theory by over-constraining the sides and angles of this triangle provides a direct test of the SM.

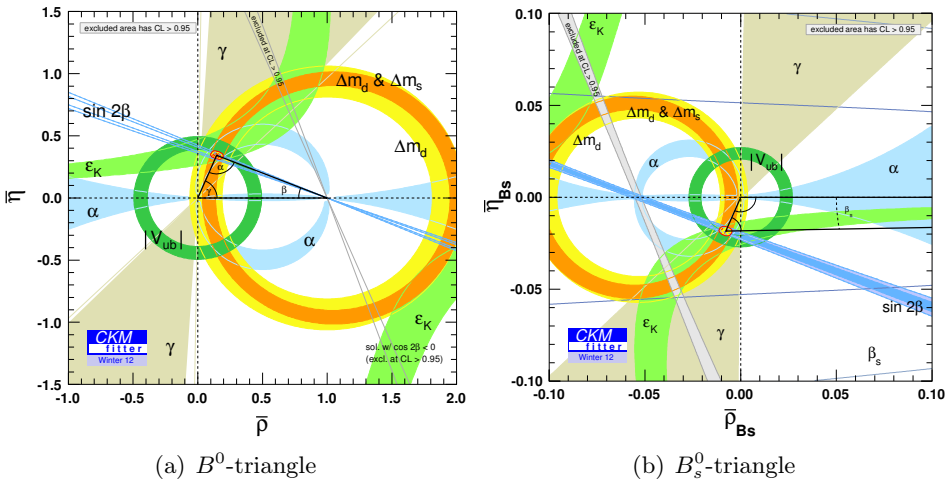


Fig. 1. Global CKM fit to the unitarity triangles.

New particles and couplings carry phases that could induce new sources of CP violation. Flavour physics is particularly sensitive to physics beyond the SM through the effects in loop diagrams, even up to high energy scales beyond the reach of direct production at the general purpose detectors.

Three types of CP violation can be distinguished. CP violation in decay where the decay rate of a  $B$  meson to a final state  $f$  is not equal to the CP conjugate process; CP violation in mixing where the probability of a  $B_{(s)}^0$  meson to oscillate to a  $\bar{B}_{(s)}^0$  meson is not equal to the probability of the CP conjugate process; and CP violation in the interference between mixing and decay. The LHCb Collaboration has performed measurements of each type of CP violation using  $B$  mesons. In this report, we will discuss

a selection of recent measurements, including the first measurement of CP violation in the  $B_s^0$ -system, a measurement of the flavour specific CP asymmetry and a measurement of the angle  $\gamma$ .

## 2. LHCb and datasets

The LHCb detector [5] is a single-arm forward spectrometer covering the pseudorapidity range  $2 < \eta < 5$ , designed for the study of particles containing  $b$  or  $c$  quarks. The detector includes a high-precision tracking system consisting of a silicon-strip vertex detector surrounding the  $pp$  interaction region, a large-area silicon-strip detector located upstream of a dipole magnet with a bending power of about 4 Tm, and three stations of silicon-strip detectors and straw drift tubes placed downstream. The combined tracking system provides a momentum measurement with relative uncertainty that varies from 0.4% at 5 GeV/ $c$  to 0.6% at 100 GeV/ $c$ , and impact parameter resolution of 20  $\mu\text{m}$  for tracks with large transverse momentum. Different types of charged hadrons are distinguished by information from two ring-imaging Cherenkov detectors. Photon, electron and hadron candidates are identified by a calorimeter system consisting of scintillating-pad and preshower detectors, an electromagnetic calorimeter and a hadronic calorimeter. Muons are identified by a system composed of alternating layers of iron and multiwire proportional chambers.

The trigger consists of a hardware stage, based on information from the calorimeter and muon systems, followed by a software stage, which applies a full event reconstruction. The software trigger requires either a dimuon pair or a two-, three- or four-track secondary vertex with a large sum of the transverse momentum,  $p_T$ , of the tracks and a significant displacement from the primary  $pp$  interaction vertices (PVs).

### 2.1. Selection of beauty events

Due to their long lifetime and large boost,  $B$  mesons typically fly a few mm before they decay. The excellent vertex resolution of the LHCb detector allows to accurately measure the separation between the primary vertex and the secondary vertex. The  $B$  meson decays discussed in this paper can be divided into three categories: charmed  $B$  meson decays, where the  $B$  meson first decays to a bachelor hadron and a charm meson with finite lifetime, that then further decays into the final state particles; charmless  $B$  meson decays, where the decay products of the  $B$  are directly produced; and semileptonic decays, with a lepton in the final state. The type of the various final state particles is determined by the RICH pion/kaon identification. Multivariate analysis, like boosted decision trees, is a commonly used

tool to separate the signal from the combinatorial background. Mass fits are used to further separate signal from background, exploiting the outstanding mass resolution of the LHCb detector.

All measurements described in this paper use the LHCb  $1 \text{ fb}^{-1}$  dataset collected in 2011 at a center-of-mass energy of 7 TeV.

### 3. CP violation in decay

CP violation in decay describes a difference in decay rate between a process and its CP-conjugate process. For CP violation in decay to occur the decay needs at least two contributions to the total decay amplitude, for instance a tree contribution and a penguin contribution. The decay rate can then be written as

$$\begin{aligned} \Gamma &\propto \left| a_{\text{T}} e^{i(\phi_{\text{T}} + \delta_{\text{T}})} + a_{\text{P}} e^{i(\phi_{\text{P}} + \delta_{\text{P}})} \right|^2 \\ &= |a_{\text{T}}|^2 + |a_{\text{P}}|^2 + 2|a_{\text{T}} a_{\text{P}}| \cos(\phi_{\text{T}} + \phi_{\text{P}} + \delta_{\text{T}} + \delta_{\text{P}}), \end{aligned} \quad (2)$$

where T refers to the tree decay path and P refers to the penguin decay path. For the CP conjugate state, the weak phase changes sign, while the strong phase keeps its original sign

$$\begin{aligned} \bar{\Gamma} &\propto \left| a_{\text{T}} e^{i(-\phi_{\text{T}} + \delta_{\text{T}})} + a_{\text{P}} e^{i(-\phi_{\text{P}} + \delta_{\text{P}})} \right|^2 \\ &= |a_{\text{T}}|^2 + |a_{\text{P}}|^2 + 2|a_{\text{T}} a_{\text{P}}| \cos(-\phi_{\text{T}} - \phi_{\text{P}} + \delta_{\text{T}} + \delta_{\text{P}}). \end{aligned} \quad (3)$$

This can be visualised by drawing the decay amplitude as a vector in the complex plane (Fig. 2 (a)). The experimental observable associated with CP violation in decay is the CP asymmetry  $A_{\text{CP}}$  which is defined as

$$A_{\text{CP}} = \frac{\Gamma(B \rightarrow f) - \Gamma(\bar{B} \rightarrow \bar{f})}{\Gamma(B \rightarrow f) + \Gamma(\bar{B} \rightarrow \bar{f})}. \quad (4)$$

#### 3.1. First measurement of CP violation in the $B_s^0$ -system, using $B_s^0 \rightarrow K^- \pi^+$ decays

The study of CP violation in charmless charged two-body decays of neutral  $B$  mesons provides stringent tests of the CKM picture in the SM, and is a sensitive probe to search for the presence of non-SM physics. The discovery of direct CP violation in the  $B^0 \rightarrow K^+ \pi^-$  decay dates back to 2004. However, CP violation has never been observed with significance exceeding five Gaussian standard deviations ( $\sigma$ ) in any  $B_s^0$  meson decay so far.

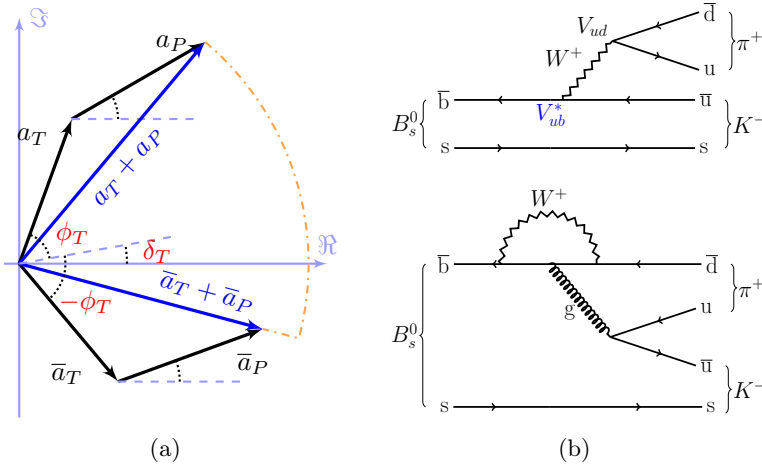


Fig. 2. (a) CP violation in decay in the complex plane. (b) Tree and penguin Feynman diagrams for the decay  $B_s^0 \rightarrow K^- \pi^+$ .

Here, we report measurements of direct CP-violating asymmetries in  $B^0 \rightarrow K^+ \pi^-$  and  $B_s^0 \rightarrow K^- \pi^+$  [6]. There are two contributions to the decay amplitude, from tree diagrams and from penguin diagrams (Fig. 2 (b)), and interference between the two decay amplitudes allows for CP violation to occur.

An untagged sample of  $B_{(s)}^0$  decays is used. A fit to the invariant mass distribution of selected events is made (Fig. 3). The event selection is optimised for  $B_s^0 \rightarrow K^- \pi^+$  and  $B^0 \rightarrow K^+ \pi^-$  separately in order to have the highest sensitivity for  $A_{CP}(B_s^0 \rightarrow K^- \pi^+)$  or  $A_{CP}(B^0 \rightarrow K^+ \pi^-)$ , respectively. The main backgrounds originate from  $B_{(s)}^0 \rightarrow K \pi$  cross feed,  $B$  to 3-body decays and combinatorial background. The signal yields extracted from the mass fit are  $N(B_s^0 \rightarrow K^- \pi^+) = 1065 \pm 55$  and  $N(B^0 \rightarrow K^+ \pi^-) = 41420 \pm 300$ . The raw asymmetries are  $A_{\text{raw}}(B_s^0 \rightarrow K^- \pi^+) = 0.28 \pm 0.04$  and  $A_{\text{raw}}(B^0 \rightarrow K^+ \pi^-) = -0.091 \pm 0.006$ , where the uncertainties are statistical only.

The raw asymmetry is equal to the CP asymmetry up to corrections for the detector asymmetry and the production asymmetry  $A_{\text{raw}} = A_{CP} - A_D - \kappa A_P$ , where  $\kappa$  is a dilution factor to take into account  $B$ -mixing. The detector asymmetry is defined as

$$A_D = \frac{\epsilon_D(K^- \pi^+) - \epsilon_D(K^+ \pi^-)}{\epsilon_D(K^- \pi^+) + \epsilon_D(K^+ \pi^-)}. \quad (5)$$

The detection asymmetry can be measured in data using calibration samples of  $D^{*+} \rightarrow D^0(K^- \pi^+) \pi^+$  and  $D^{*+} \rightarrow D^0(K^- K^+) \pi^+$  decays. The combi-

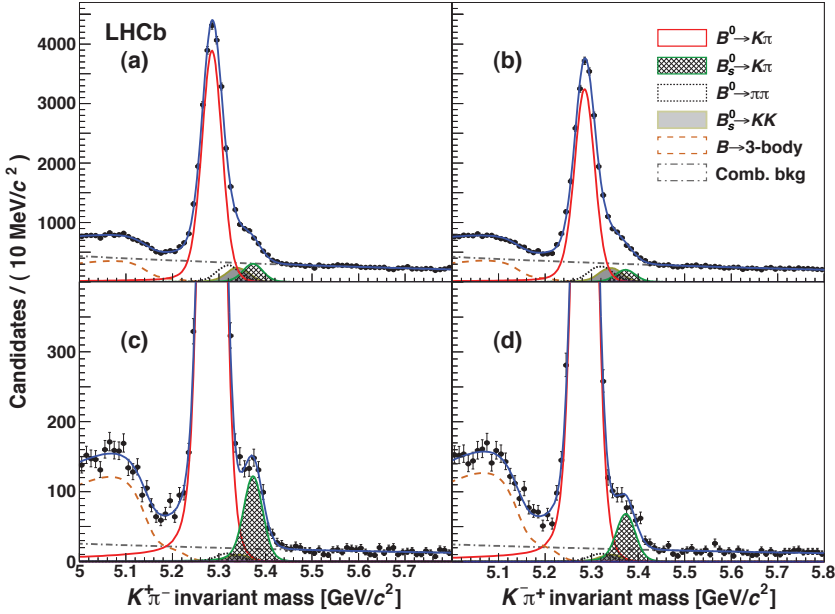


Fig. 3. Invariant mass spectra obtained using the event selection adopted for the best sensitivity on (a), (b)  $A_{\text{CP}}(B^0 \rightarrow K^+\pi^-)$  and (c), (d)  $A_{\text{CP}}(B_s^0 \rightarrow K^-\pi^+)$ . Panels (a) and (c) represent the  $K^+\pi^-$  invariant mass, whereas panels (b) and (d) represent the  $K^-\pi^+$  invariant mass. Figure from Ref. [6].

nation of the time-integrated raw asymmetries of these two decay modes is used to disentangle the detection asymmetry for  $K\pi$ . The raw asymmetries measured in the calibration samples can be written as

$$A_{\text{raw}}^*(K\pi) = A_{\text{D}}^*(\pi_s) + A_{\text{P}}(D^*) + A_{\text{D}}^*(K\pi), \quad (6)$$

$$A_{\text{raw}}^*(KK) = A_{\text{D}}^*(\pi_s) + A_{\text{P}}(D^*) + A_{\text{CP}}(KK). \quad (7)$$

By subtracting Eqs. (6) and (7), one obtains

$$A_{\text{raw}}^*(K\pi) - A_{\text{raw}}^*(KK) = A_{\text{D}}^*(K\pi) - A_{\text{CP}}(KK), \quad (8)$$

where  $A_{\text{raw}}^*(K\pi)$  and  $A_{\text{raw}}^*(KK)$  are the time-integrated raw asymmetries in the  $D^*$ -tagged  $D^0 \rightarrow K^-\pi^+$  and  $D^0 \rightarrow K^-K^+$  decays,  $A_{\text{CP}}(KK)$  is  $D^0 \rightarrow K^-K^+$  CP asymmetry, and  $A_{\text{D}}^*(K\pi)$  is the detection asymmetry in reconstructing  $D^0 \rightarrow K^-\pi^+$  and  $\bar{D}^0 \rightarrow K^+\pi^-$  decays. After correcting for differences in kinematic properties between the  $D$  and the  $B$  meson, we find  $A_{\text{D}}(K\pi) = (-1.15 \pm 0.23)\%$  for the  $B_s^0$  sample and  $A_{\text{D}}(K\pi) = (-1.22 \pm 0.21)\%$  for the  $B^0$  sample.

The production asymmetry can be measured exploiting the time dependence of the decay. Assuming negligible CP violation in mixing, as is expected in the SM, the time dependent CP asymmetry can be written as

$$\mathcal{A}(t) \approx A_{\text{CP}} + A_{\text{D}} + A_{\text{P}} \cos(\Delta m_{s(d)} t). \quad (9)$$

The amplitude of the oscillation is given by the production asymmetry. By studying the full time-dependent decay rate, it is then possible to determine  $A_{\text{P}}$  unambiguously. We find for the production asymmetry  $A_{\text{P}}(B_s^0) = (4 \pm 8)\%$  and  $A_{\text{P}}(B^0) = (0.1 \pm 1.0)\%$ . The raw asymmetries are shown in Fig. 4.

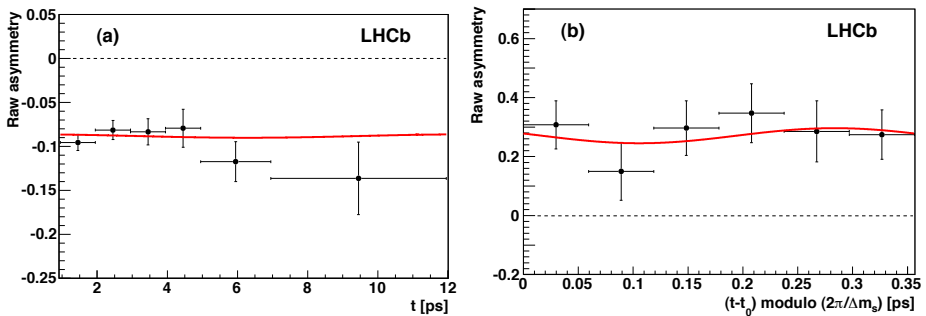


Fig. 4. Time dependent CP asymmetry for (a)  $B^0 \rightarrow K^+\pi^-$  and (b)  $B_s^0 \rightarrow K^-\pi^+$ . Figures from Ref. [6].

Combining the ingredients discussed above, the CP asymmetry measured with  $B_s^0 \rightarrow K^-\pi^+$  and  $B^0 \rightarrow K^+\pi^-$  decays is

$$A_{\text{CP}}(B_s^0 \rightarrow K^-\pi^+) = 0.27 \pm 0.04 (\text{stat.}) \pm 0.01 (\text{syst.}), \quad (10)$$

$$A_{\text{CP}}(B^0 \rightarrow K^+\pi^-) = -0.080 \pm 0.007 (\text{stat.}) \pm 0.003 (\text{syst.}), \quad (11)$$

where the largest contribution to the systematic uncertainty comes from the cross-feed background and the detection asymmetry. This is the first observation, with  $6.5\sigma$ , of CP violation in the  $B_s^0$  system, and the most precise measurement of  $A_{\text{CP}}(B^0 \rightarrow K^+\pi^-)$  to date. The two measurements provide a test of the SM, which predicts the ratio of CP asymmetries for  $B^0$  and  $B_s^0$  to be equal to the ratio of partial decay widths

$$\Delta = \frac{A_{\text{CP}}(B^0 \rightarrow K^+\pi^-)}{A_{\text{CP}}(B_s^0 \rightarrow K^-\pi^+)} + \frac{\mathcal{B}(B_s^0 \rightarrow K^-\pi^+)}{\mathcal{B}(B^0 \rightarrow K^+\pi^-)} \frac{\tau_d}{\tau_s} = 0. \quad (12)$$

The value found by LHCb  $\Delta = -0.02 \pm 0.05 \pm 0.04$  is consistent with the SM prediction.

3.2. New mechanisms for CP violation, using  $B^\pm \rightarrow h^+h^-\pi^\pm$  decays

Charmless decays of  $B$  mesons to three hadrons are dominated by quasi-two-body processes involving intermediate resonant states. The rich interference pattern present in such decays makes them favourable for the investigation of charge asymmetries that are localised in the phase space. For CP violation in decay to occur, two interfering amplitudes with different weak and strong phases must be involved in the decay process. Interference between intermediate states of the decay can introduce large strong phase differences, and is one mechanism for explaining local asymmetries in the phase space. Another explanation focuses on final-state  $KK \leftrightarrow \pi\pi$  rescattering.

Here, a measurement of CP violation in decay using the decay  $B^\pm \rightarrow h^+h^-\pi^\pm$  is reported, where  $h$  is either a pion or a kaon [7]. Interference between tree and penguin contributions to the decay amplitude (Fig. 5) allows for CP violation to occur. The measured asymmetry is related to the CP asymmetry as  $A_{\text{raw}} = A_{\text{CP}} - A_{\text{D}} - A_{\text{P}}$ . The detection asymmetry is measured to be  $A_{\text{D}} = -0.010 \pm 0.007$  and the production asymmetry is measured using  $B^\pm \rightarrow J/\psi(\mu\mu)K^\pm$  decays to be  $A_{\text{P}} = -0.004 \pm 0.004$ .

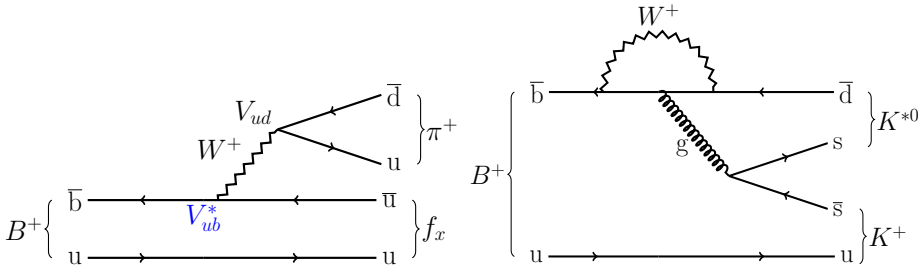


Fig. 5. Feynman diagrams describing two contributions to the decay amplitude of  $B^\pm \rightarrow K^+K^-\pi^\pm$ .  $f_x$  denotes any resonance that decays to two kaons in the final state.

The raw asymmetry is measured using selected events by fitting the  $h^+h^-\pi^\pm$  invariant mass distribution (Fig. 6). The main backgrounds are from  $B_{(s)}^0$  4-body decays and combinatorial background. The signal yields are  $N(KK\pi) = 1870 \pm 133$  and  $N(\pi\pi\pi) = 4904 \pm 148$ . From these, the CP asymmetries are determined to be  $A_{\text{CP}}(B^\pm \rightarrow K^+K^-\pi^\pm) = -0.141 \pm 0.040 \pm 0.018 \pm 0.007$  and  $A_{\text{CP}}(B^\pm \rightarrow \pi^+\pi^-\pi^\pm) = 0.117 \pm 0.021 \pm 0.009 \pm 0.007$ , where the first uncertainty is statistical, the second is systematic, and the third is due to the CP asymmetry of the  $B^\pm \rightarrow J/\psi K^\pm$  reference mode. The largest contributions to the systematic uncertainty are from the acceptance and from differences in kinematics between kaons from  $B$  and  $D$  decays, which enters in the determination of the detection asymmetry.

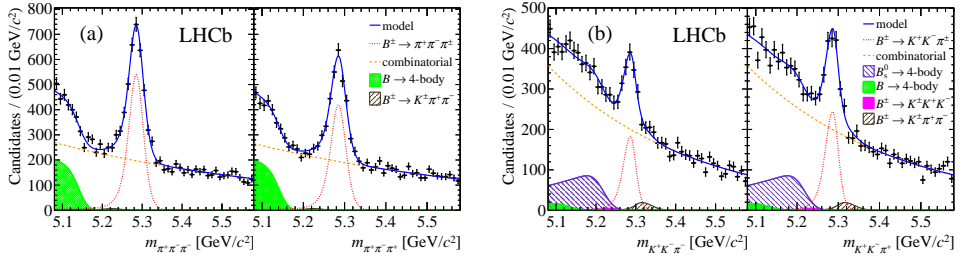


Fig. 6. Invariant mass distribution of (a)  $B^\pm \rightarrow \pi^+\pi^-\pi^\pm$  and (b)  $B^\pm \rightarrow K^+K^-\pi^\pm$  decays. Figures from Ref. [7].

The raw asymmetry has been studied in the 2-dimensional Dalitz plane (Fig. 7), where the binning is defined such that each bin contains roughly an equal number of  $B$  events. A local asymmetry is found in the  $B^\pm \rightarrow \pi^+\pi^-\pi^\pm$  Dalitz plane in the region  $m_{\pi^+\pi^-\text{low}}^2 < 0.4 \text{ GeV}^2/c^4$  and  $m_{\pi^+\pi^-\text{high}}^2 > 15 \text{ GeV}^2/c^4$ . For  $B^\pm \rightarrow K^+K^-\pi^\pm$  decays, a local negative asymmetry is found for  $m_{K^+K^-}^2 < 1.5 \text{ GeV}^2/c^4$ . The CP asymmetries are further studied in these regions, by fitting the 3-body invariant mass spectra in these regions. The two local charge asymmetries are found to be  $A_{\text{CP}}^{\text{loc}}(B^\pm \rightarrow \pi^+\pi^-\pi^\pm) = 0.584 \pm 0.082 \pm 0.027 \pm 0.007$  and  $A_{\text{CP}}^{\text{loc}}(B^\pm \rightarrow K^+K^-\pi^\pm) = -0.648 \pm 0.070 \pm 0.013 \pm 0.007$ , where the first uncertainty is statistical, the second is systematic, and the third is due to the CP asymmetry of the  $B^\pm \rightarrow J/\psi K^\pm$  reference mode.

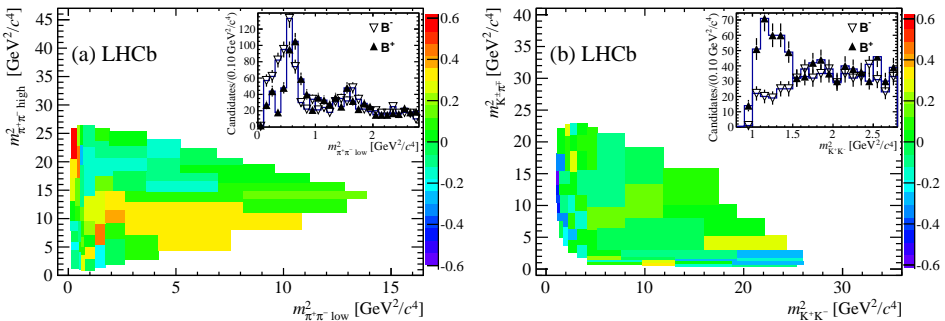


Fig. 7. Raw asymmetry in the Dalitz plane for (a)  $B^\pm \rightarrow \pi^+\pi^-\pi^\pm$  and (b)  $B^\pm \rightarrow K^+K^-\pi^\pm$  decays. Localised regions with large asymmetries are observed. Figures from Ref. [7].

First evidence of CP violation in decay has been found in the decays  $B^\pm \rightarrow \pi^+\pi^-\pi^\pm$  ( $4.9\sigma$ ) and  $B^\pm \rightarrow K^+K^-\pi^\pm$  ( $3.2\sigma$ ). A localised region with large  $A_{\text{CP}}$  has been found for  $B^\pm \rightarrow \pi^+\pi^-\pi^\pm$  decays, that is not clearly

associated to a resonant state. Also for  $B^\pm \rightarrow K^+K^-\pi^\pm$  decays, a large localised asymmetry is measured, where no significant resonant contribution is expected.

### 3.3. Measurement of $\gamma$ with trees, using $B^\pm \rightarrow D^0 h^\pm$ decays

A precise determination of the unitarity triangle angle  $\gamma$  is an important goal in flavour physics, as it is to date the least well known angle of the triangle. The angle  $\gamma$  is defined as  $\gamma = \arg[-V_{ud}V_{ub}^*/(V_{cd}V_{cb}^*)]$ , where  $V_{ij}$  are the elements of the CKM matrix. A measurement of  $\gamma$  in processes involving only tree-level decays provides a SM benchmark against which observables more sensitive to new physics contributions can be compared. Moreover, a measurement of  $\gamma$  over-constrains the unitarity triangle and provides a test of the SM. Here, we report on a combination of three measurements done by the LHCb Collaboration [8]. The three individual measurements, each using  $B^\pm \rightarrow D^0 K^\pm$  and  $B^\pm \rightarrow D^0 \pi^\pm$  decays with different  $D^0$  decay modes, are discussed briefly in the following sections. A frequentist approach is used for the combination of the measurements. A combined likelihood of the experimental observables is constructed and the full information of the covariance matrices is included. Also  $D^0$  mixing is taken into account. The following value for the angle  $\gamma$  extracted

$$\begin{aligned} \gamma &= 72.6^\circ && \text{(central value)} \\ \gamma &\in [55.4, 82.3]^\circ && \text{at 68\% C.L.} \end{aligned} \quad (13)$$

and is limited by the statistical uncertainty (Fig. 8). A preliminary result that includes updated results of the GGSZ analysis (see below) using the 2012 LHCb dataset [9] is available and finds a central value of  $\gamma = 67.2^\circ$  with a 68% confidence level range of  $[55.1, 79.1]$ .

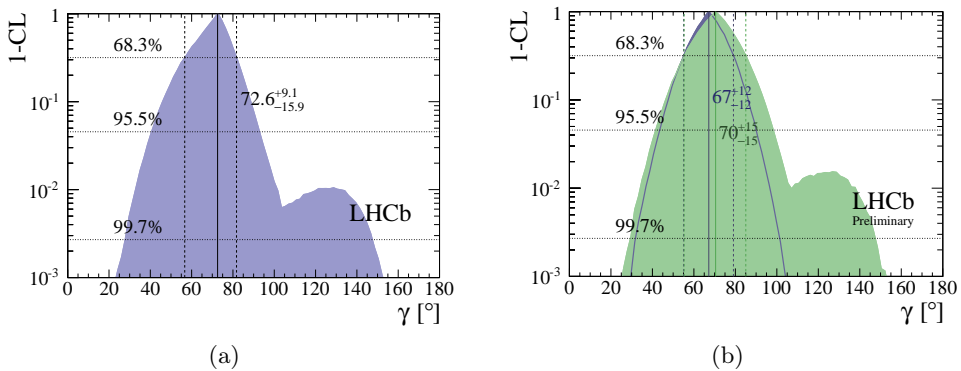


Fig. 8. 1-C.L. graphs for  $\gamma$ . (a) Full combination, figure from Ref. [8]; (b) Update, using only  $B^\pm \rightarrow D^0 K^\pm$  decays, figure from Ref. [9].

### 3.3.1. GLW method

The first measurement included in the combination uses  $B^\pm \rightarrow D^0 h^\pm$  decays, where the  $D^0$  decays to a CP-eigenstate, for instance  $K^+K^-$  or  $\pi^+\pi^-$  [10]. This method was first proposed by Gronau, London, and Wyler in 1991 [11, 12] and is denoted GLW. The advantage of this method is that the event rates are large.

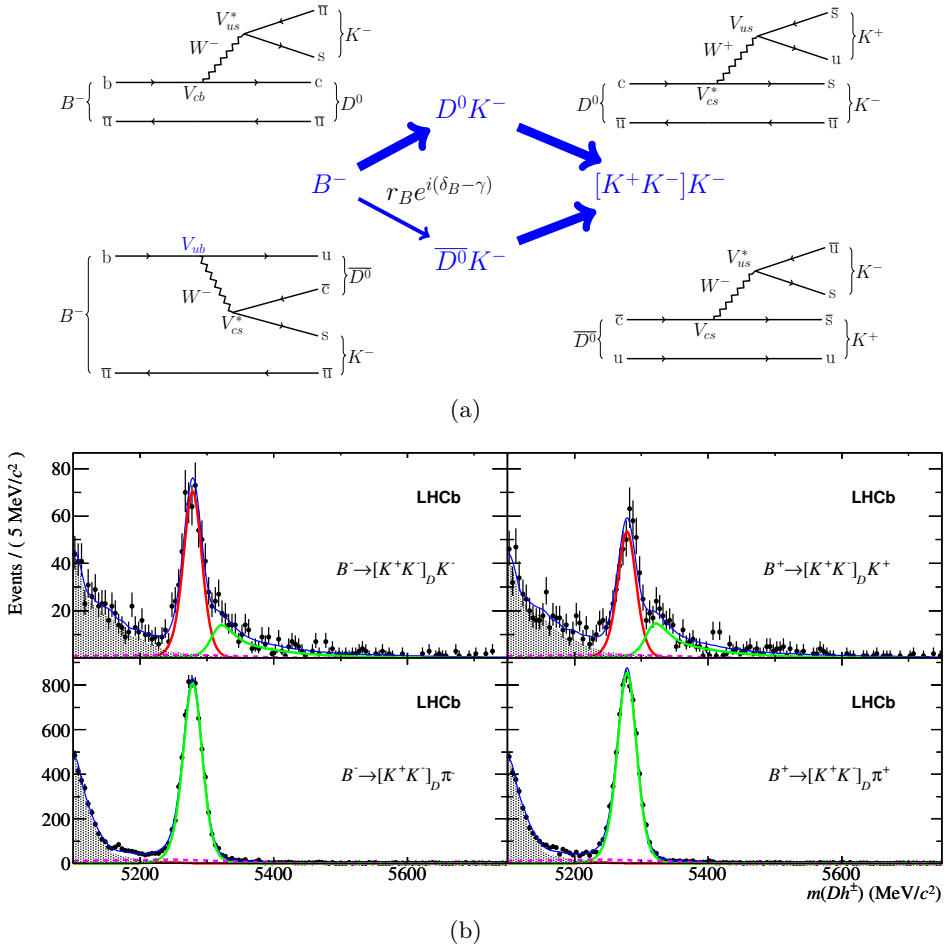


Fig. 9. (a) shows the different decay paths accessible to the decay  $B^- \rightarrow (K^+K^-)K^-$ . The thickness of the arrow represents the size of the decay amplitude. (b) Invariant mass distribution of  $B^\pm \rightarrow (K^+K^-)h^\pm$  decays. Figure from Ref. [10].

However, the interference is small due to the Cabibbo suppression of one of the decay paths (Fig. 9 (a)). There are two observables, a CP asymmetry defined as

$$\begin{aligned} A_{\text{CP}^+} &= \frac{\Gamma(B^- \rightarrow f_D K^-) - \Gamma(B^+ \rightarrow f_D K^+)}{\Gamma(B^- \rightarrow f_D K^-) + \Gamma(B^+ \rightarrow f_D K^+)} \\ &= \frac{2r_B \sin \delta_B \sin \gamma}{1 + r_B^2 + 2r_B \cos \delta_B \cos \gamma} \end{aligned} \quad (14)$$

and a ratio of decay rates

$$\begin{aligned} R_{\text{CP}^+} &= \frac{\Gamma(B^- \rightarrow f_{D,\text{CP}} K^-) + \Gamma(B^+ \rightarrow f_{D,\text{CP}} K^+)}{\Gamma(B^- \rightarrow f_{D,\text{tot}} K^-) + \Gamma(B^+ \rightarrow f_{D,\text{tot}} K^+)} \\ &= 1 + r_B^2 + 2r_B \cos \delta_B \cos \gamma. \end{aligned} \quad (15)$$

The three parameters in these equations are the ratio of the amplitudes of the two decay paths  $r_B$ , a strong phase  $\delta_B$  associated with the  $B^\pm \rightarrow D^0 h^\pm$  decay and the weak phase  $\gamma$ .

The observables  $A_{\text{CP}^+}$  and  $R_{\text{CP}^+}$  are measured by exploiting the invariant mass distribution of  $B^\pm \rightarrow D^0(h^+h^-)h^\pm$  candidates. Figure 9 (b) shows a clear charge asymmetry for  $B^\pm \rightarrow D^0(K^+K^-)K^\pm$  decays. This measurement does not yield enough information to extract the angle  $\gamma$ . Therefore, a second group of measurements is introduced.

### 3.3.2. ADS method

The second measurement included in the combination uses  $B^\pm \rightarrow D^0 h^\pm$  decays, where the  $D^0$  decays to a final state which is common to the  $D^0$  and the  $\bar{D}^0$ , for instance  $K^\pm \pi^\pm$  [10] or  $K^\pm \pi^\pm \pi^+ \pi^-$  [13]. This method was first proposed by Atwood, Dunietz, and Soni in 1997 [14, 15] and is denoted ADS. The disadvantage of this method is that the event rates are small. However, due to a suppression of both decay paths, the decay amplitudes of the two decay paths is of comparable size, leading to a large interference (Fig. 10 (a)). There are two observables, a CP asymmetry defined as

$$\begin{aligned} A_{\text{ADS}} &= \frac{\Gamma(B^- \rightarrow f_D K^-) - \Gamma(B^+ \rightarrow \bar{f}_D K^+)}{\Gamma(B^- \rightarrow f_D K^-) + \Gamma(B^+ \rightarrow \bar{f}_D K^+)} \\ &= \frac{2r_B r_D \sin(\delta_B + \delta_D) \sin \gamma}{r_B^2 + r_D^2 + 2r_B r_D \cos(\delta_B + \delta_D) \cos \gamma} \end{aligned} \quad (16)$$

and a ratio of decay rates

$$\begin{aligned} R_{\text{ADS}} &= \frac{\Gamma(B^- \rightarrow f_D K^-) + \Gamma(B^+ \rightarrow \bar{f}_D K^+)}{\Gamma(B^- \rightarrow \bar{f}_D K^-) + \Gamma(B^+ \rightarrow f_D K^+)} \\ &= r_B^2 + r_D^2 + 2r_B r_D \cos(\delta_B + \delta_D) \cos \gamma. \end{aligned} \quad (17)$$

The five parameters in these equations are the ratio of the amplitudes of the two decay paths  $r_B$ , a strong phase  $\delta_B$  associates with the  $B^\pm \rightarrow D^0 h^\pm$  decay and the weak phase  $\gamma$ , that we already saw before. In addition, the phase  $\delta_D$  is associated with the  $D^0 \rightarrow h^+ h^-$  decay, while the ratio  $r_D$  describes the ratio of decay amplitudes for the  $D^0 \rightarrow K^- \pi^+$  decay.

The observables  $A_{\text{ADS}}$  and  $R_{\text{ADS}}$  are measured by exploiting the invariant mass distribution of  $B^\pm \rightarrow D^0(h^+ h^-)h^\pm$  candidates. Figure 10 (b) shows a clear charge asymmetry for  $B^\pm \rightarrow D^0(\pi^+ K^-)K^\pm$  decays. Combined with the measurements of the GLW type, these measurements yield enough information to extract the angle  $\gamma$ .

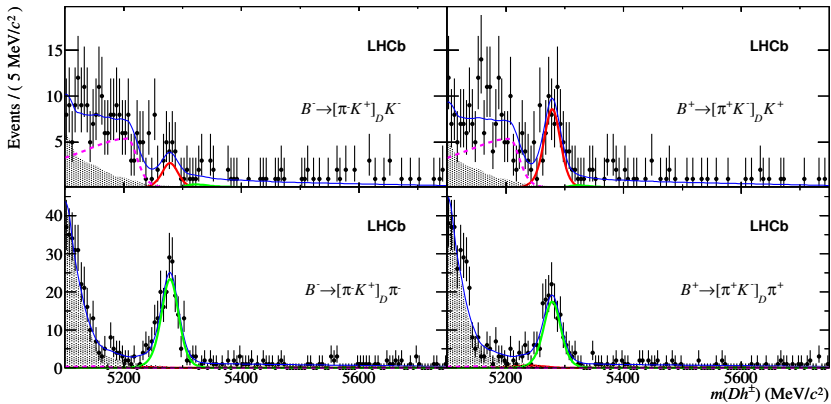
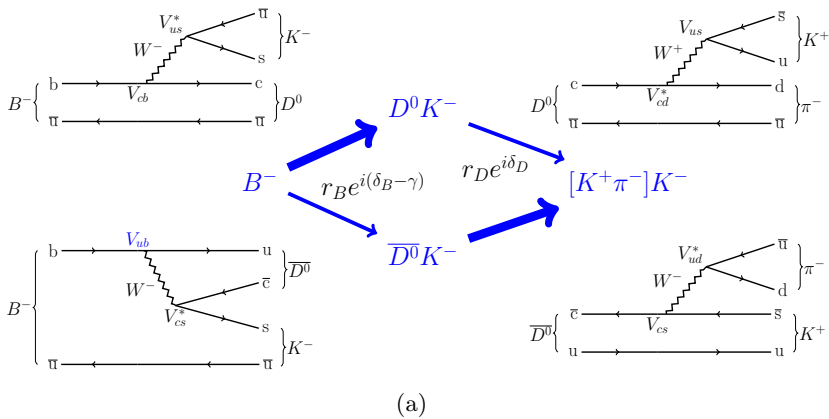


Fig. 10. (a) shows the different decay paths accessible to the decay  $B^- \rightarrow (\pi^- \pi^+)K^-$ . The thickness of the arrow represents the size of the decay amplitude. (b) Invariant mass distribution of  $B^\pm \rightarrow (\pi^- \pi^+)h^\pm$  decays. Figure from Ref. [10].

**3.3.3. GGSZ method**

To increase sensitivity to the angle  $\gamma$ , a third measurement is added to the combination. This measurement uses  $D^0$  decays where the final state is accessible to both the  $D^0$  and the  $\bar{D}^0$ . Moreover, it uses decays where the  $D^0$  decay exhibits a structure in the Dalitz plane [16]. The use of final states  $K_S^0 h^+ h^-$ , where  $h$  is either a pion or a kaon, was first proposed by Giri, Grossman, Soffer and Zupan in 2003 [17], and is denoted GGSZ. The decay amplitude of  $B^\pm \rightarrow (K_S^0 h^+ h^-) K^\pm$  decays can be written as a superposition of  $B^\pm \rightarrow D^0 K^\pm$  and  $B^\pm \rightarrow \bar{D}^0 K^\pm$  decays

$$A_B(m_+^2, m_-^2) = f + r_B e^{i(\delta_B - \gamma)} \bar{f}, \tag{18}$$

where  $m_+^2$  and  $m_-^2$  are the invariant masses squared of the  $K_S^0 h^+$  and  $K_S^0 h^-$  combinations that define the position in the Dalitz plane,  $f$  is the  $D^0 \rightarrow K_S^0 h^+ h^-$  decay amplitude and  $\bar{f}$  is the  $\bar{D}^0 \rightarrow K_S^0 h^+ h^-$  decay amplitude.

In the Dalitz plane of  $B^\pm \rightarrow D^0(h^+ h^-) h^\pm$  decays, a different structure can be identified in the  $B^+$  plane compared to the  $B^-$  plane (Fig. 11). The Dalitz plot is partitioned into  $2N$  regions that are symmetric under the exchange  $m_+^2 \leftrightarrow m_-^2$ . The decay equations for bin  $i$  are given by

$$\Gamma_{\pm i}(B^-) = h_{B^-} \left[ K_{\pm i} + r_B^2 K_{\mp i} + 2\sqrt{K_{-i}, K_{+i}}(x_- c_{\pm i} + y_- s_{\pm i}) \right], \tag{19}$$

$$\Gamma_{\pm i}(B^+) = h_{B^+} \left[ K_{\mp i} + r_B^2 K_{\pm i} + 2\sqrt{K_{-i}, K_{+i}}(x_+ c_{\pm i} - y_+ s_{\pm i}) \right], \tag{20}$$

where the parameters  $K$ ,  $c$  and  $s$  have their origin in the decay  $D^0 \rightarrow K_S^0 h^+ h^-$ , while the parameters  $x_\pm$  and  $y_\pm$  are related to the  $B^\pm \rightarrow D^0 K^\pm$

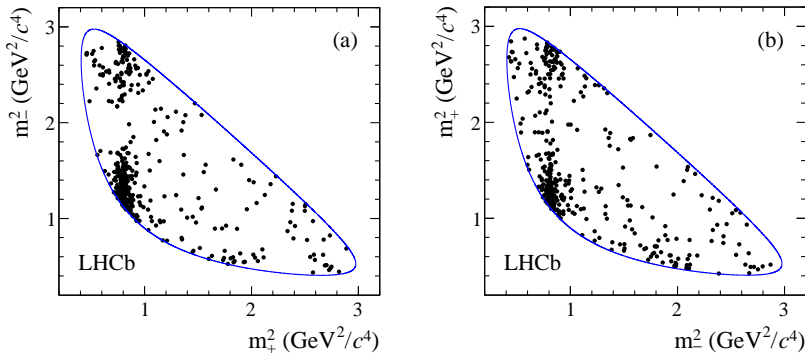


Fig. 11. Dalitz plots of  $B^\pm \rightarrow D^0 K^\pm$  candidates in the signal region for  $D^0 \rightarrow K_S^0 \pi^+ \pi^-$  decays, where (a) is  $B^+$  and (b) is  $B^-$ . The boundaries of the kinematically-allowed regions are also shown. Figure from Ref. [16].

decay. The information about the angle  $\gamma$  is contained in the parameters  $x_{\pm}$  and  $y_{\pm}$ , which are given by

$$x_{\pm} = r_B \cos(\delta_B \pm \gamma), \tag{21}$$

$$y_{\pm} = r_B \sin(\delta_B \pm \gamma). \tag{22}$$

For the parameters  $K$ ,  $c$  and  $s$  external input is used from the CLEO Collaboration. The parameters  $x_{\pm}$  and  $y_{\pm}$  are determined by LHCb by exploiting the structure in the Dalitz plane.

#### 4. CP violation in mixing

CP violation in mixing occurs when the probability of a  $B$  meson to oscillate to a  $\bar{B}$  meson is not equal to the probability of the CP conjugate process

$$\text{Prob} \left( B_{(s)}^0 \rightarrow \bar{B}_{(s)}^0 \right) \neq \text{Prob} \left( \bar{B}_{(s)}^0 \rightarrow B_{(s)}^0 \right). \tag{23}$$

The oscillation of a  $B$  meson to a  $\bar{B}$  meson can go either via off-shell states (box diagrams) or via on-shell states, where the  $B$  meson decays to an intermediate state  $f$  and then oscillates back to a  $\bar{B}$  meson. There can be a relative phase between the on- and off-shell states

$$\phi_{12} \equiv \arg \left( \frac{M_{12}}{\Gamma_{12}} \right). \tag{24}$$

If  $\phi_{12}$  is not zero, there is CP violation in mixing. This means that the  $B$ -heavy and the  $B$ -light states are not composed of equal contributions of  $B$  and  $\bar{B}$ , and thus that  $q/p$  is not equal to unity

$$\frac{q}{p} = -\sqrt{\frac{M_{12}^* - \frac{i}{2}\Gamma_{12}^*}{M_{12} - \frac{i}{2}\Gamma_{12}}} \neq 1. \tag{25}$$

##### 4.1. Measurement of the phase $\phi_{12}$ , using $B_s^0 \rightarrow D_s^- \mu^+ \nu$ decays

The SM prediction of the phase  $\phi_{12} \approx 0.2^\circ$  which makes it a sensitive probe to new physics. The flavour specific CP violating asymmetry related to  $\phi_{12}$  is

$$a_{\text{sl}} = 1 - \left| \frac{q}{p} \right|^2 \approx \frac{\Delta\Gamma}{\Delta M} \tan \phi_{12}. \tag{26}$$

This CP asymmetry can be measured using  $B_s^0 \rightarrow D_s^- \mu^+ \nu$  decays [18]. We measure an untagged final state asymmetry, which is related to  $a_{\text{sl}}$  following

$$\begin{aligned} A_{\text{meas}} &= \frac{\Gamma[D_s^- \mu^+] - \Gamma[D_s^+ \mu^-]}{\Gamma[D_s^- \mu^+] + \Gamma[D_s^+ \mu^-]} \\ &= \frac{a_{\text{sl}}^s}{2} + \left[ A_{\text{P}} - \frac{a_{\text{sl}}^s}{2} \right] \frac{\int_{t=0}^{\infty} e^{-\Gamma_s t} \cos(\Delta M_s t) \epsilon(t) dt}{\int_{t=0}^{\infty} e^{-\Gamma_s t} \cosh\left(\frac{\Delta \Gamma_s t}{2}\right) \epsilon(t) dt}, \end{aligned} \quad (27)$$

where  $A_{\text{P}}$  is the production asymmetry which is approximately 1%,  $\epsilon(t)$  is the decay time acceptance function and  $\Gamma_s$  is the average decay width of the  $B_s^0\text{-}\bar{B}_s^0$  meson system. Due to the large value of the mass difference,  $\Delta M_s = 17.768 \pm 0.024 \text{ ps}^{-1}$  [19], the oscillations are rapid and the integral ratio in Eq. (27) is approximately 0.2%. This is well below the desired precision, and thus can be neglected, yielding  $A_{\text{meas}} = 0.5 a_{\text{sl}}$ .

There are three contributions to the measured asymmetry,  $A_{\text{meas}} = A_{\mu}^c - A_{\text{track}} - A_{\text{bkg}}$ , where the first term is the measured yield asymmetry corrected for muon PID and trigger efficiency, the second term is a charge asymmetry due to track reconstruction, and the third term is a charge asymmetry due to backgrounds. The yield asymmetry is defined as

$$A_{\mu}^c = \frac{N(D_s^+ \mu^-)/\epsilon(\mu^-) - N(D_s^- \mu^+)/\epsilon(\mu^+)}{N(D_s^+ \mu^-)/\epsilon(\mu^-) + N(D_s^- \mu^+)/\epsilon(\mu^+)} \quad (28)$$

and is obtained from a fit to the invariant mass spectrum of  $D_s$  candidates (Fig. 12 (a)). The muon trigger and PID efficiencies are measured in data using a sample of  $J/\psi \rightarrow \mu^+ \mu^-$  decays. The muon efficiency is found to be momentum independent with a residual asymmetry due to the alignment of the muon stations.

The asymmetry due to track reconstruction can be decomposed in two parts  $A_{\text{track}} = A_{\text{track}}^{\pi\mu} + A_{\text{track}}^{KK}$ . The  $\mu$  and  $\pi$  charged tracks have very similar reconstruction efficiencies. Using a calibration sample of partially reconstructed  $D^{*+}$  decays, we found that the  $\pi^+$  versus  $\pi^-$  relative tracking efficiencies are independent of momentum and transverse momentum. In the  $K^+ K^- \pi^- \mu^+$  final states, the pion and muon have opposite sign, and thus the charge asymmetry in the track reconstruction efficiency induced by pions and muons is small. A small residual sensitivity to the charge asymmetry in kaon track reconstruction is present due to a slight momentum mismatch between the two kaons from  $\phi$  decays arising from the interference with the S-wave component. The total asymmetry due to the track reconstruction is found to be  $A_{\text{track}} = (+0.02 \pm 0.13)\%$ .

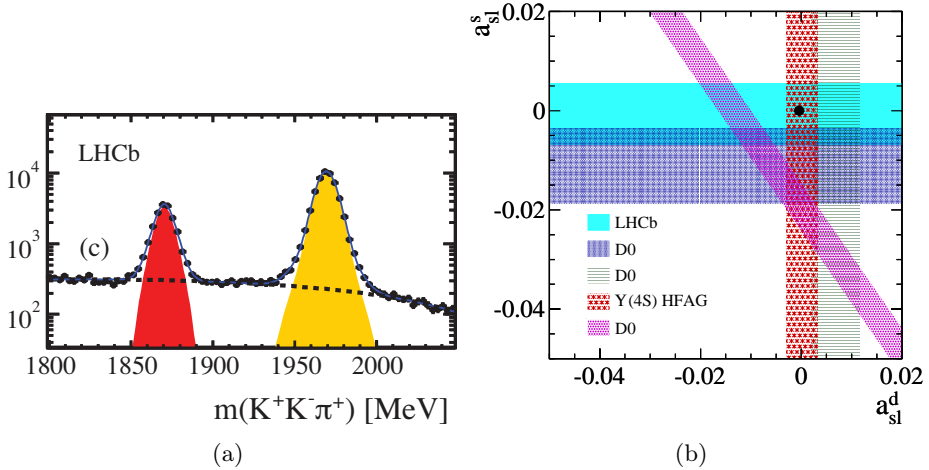


Fig. 12. (a) invariant mass distribution of  $D_s^+$  candidates. The light grey/yellow peak corresponds to the signal. (b) Measurements of semileptonic decay asymmetries. The bands correspond to the central values  $\pm 1$  standard deviation uncertainties. The plain grey/blue band depicts the measurement done by LHCb, whereas the SM prediction is the black dot. Figures from Ref. [18].

The last component of the measured asymmetry is an asymmetry due to the presence of various backgrounds. These backgrounds can be different in the  $D_s^- \mu^+$  sample compared to the  $D_s^+ \mu^-$  sample. Three sources of background need to be taken into account. There is a background from prompt charm decays, where a prompt  $D_s$  is combined with a random muon. Secondly, there is a background from misidentified  $b$ -hadron decays, where a pion or a kaon is identified as a muon. The last background is from  $B \rightarrow DD_s$  decay, where the  $D$  decays semileptonically. The total asymmetry due to the background is found to be  $A_{\text{bkg}} = (+0.05 \pm 0.05)\%$ .

The value of the flavour specific CP asymmetry measured by the LHCb Collaboration is  $a_{\text{sl}}^s = (-0.06 \pm 0.50 \pm 0.36)\%$  (Fig. 12), and is in agreement with the SM.

## 5. CP violation in interference between mixing and decay

CP violation in decay occurs when the decay amplitudes of two CP conjugate states ( $A_f$  and  $\bar{A}_f$ ) differ. CP violation in mixing occurs when  $q/p \neq 1$ . To study CP violation in the interference between mixing and decay, we need to look at the phase difference between the two:  $\Im \lambda_f \neq 0$ , where  $\lambda_f = \frac{q}{p} \frac{\bar{A}_f}{A_f}$ . Note that there can be CP violation in interference between mixing and decay, without there being CP violation in mixing or decay.  $B$  meson decays to a flavour specific final state do not exhibit any CP violation in interference, because  $\bar{A}_f = 0$ .

The decay equations for a  $B_s^0$  decay into a CP eigenstate are given by

$$\begin{aligned} \Gamma(B_s^0 \rightarrow f)(t) &\propto |A_f|^2 (1 + |\lambda_f|^2) [\cosh(\Delta\Gamma_s t) + D_f \sinh(\Delta\Gamma_s t) \\ &\quad + C_f \cos(\Delta m_s t) - S_f \sin(\Delta m_s t)] , \\ \Gamma(\bar{B}_s^0 \rightarrow f)(t) &\propto \left| \frac{q}{p} \right| |A_f|^2 (1 + |\lambda_f|^2) [\cosh(\Delta\Gamma_s t) + D_f \sinh(\Delta\Gamma_s t) \\ &\quad - C_f \cos(\Delta m_s t) + S_f \sin(\Delta m_s t)] . \end{aligned} \quad (29)$$

One can identify a CP-even part, given by the hyperbolic functions, which do not change sign when CP conjugation is applied to the initial state. The CP-odd part, the cosine and the sine, does change sign when CP conjugation is applied to the initial state. The information on the CP violating phase is contained in the coefficients  $D$ ,  $C$ , and  $S$ , which are defined as

$$C_f = \frac{1 - |\lambda_f|^2}{1 + |\lambda_f|^2}, \quad S_f = \frac{2\Im\lambda_f}{1 + |\lambda_f|^2}, \quad D_f = \frac{2\Re\lambda_f}{1 + |\lambda_f|^2}. \quad (30)$$

### 5.1. Measurement of $\gamma$ with loops, using $B_s^0 \rightarrow K^- K^+$ decays

The study of the decay  $B_s^0 \rightarrow K^- K^+$  provides a test of the CKM picture of the SM, as it yields sensitivity to the angle  $\gamma$ . In addition, it is sensitive to new physics, as new particles can contribute to the penguin amplitude (Fig. 13 (a)).

Here, we report on a measurement of CP observables using the decay  $B_s^0 \rightarrow K^- K^+$  [20]. The decay time equations for this decay, taking into account all experimental factors, can be written as

$$\begin{aligned} f(t, \xi) &= K \{ [(1 - A_P) \Omega_\xi^B + (1 + A_P) \bar{\Omega}_\xi^B] I_+(t) \\ &\quad + [(1 - A_P) \Omega_\xi^B - (1 + A_P) \bar{\Omega}_\xi^B] I_-(t) \} \end{aligned} \quad (31)$$

with

$$\begin{aligned} I_+(t) &= \{ e^{-\Gamma_s t} [\cosh(\Delta\Gamma_s t/2) + D_f \sinh(\Delta\Gamma_s t/2)] \} \otimes R(t) \varepsilon_{\text{acc}}(t) , \\ I_-(t) &= \{ e^{-\Gamma_s t} [C_f \cos(\Delta m_s t) - S_f \sin(\Delta m_s t)] \} \otimes R(t) \varepsilon_{\text{acc}}(t) , \end{aligned} \quad (32)$$

where  $A_P$  is the production asymmetry,  $\Omega_\xi^B$  gives the probability to tag a  $B_s^0$  as a  $B_s^0$ ,  $R(t)$  is a resolution model,  $\varepsilon_{\text{acc}}(t)$  is an acceptance function,  $K$  is an overall normalisation, and  $S_f$ ,  $C_f$  and  $D_f$  are the observables as defined in Eq. (30). The various experimental factors will be briefly discussed in the lines below. An extensive discussion can be found in Ref. [20].

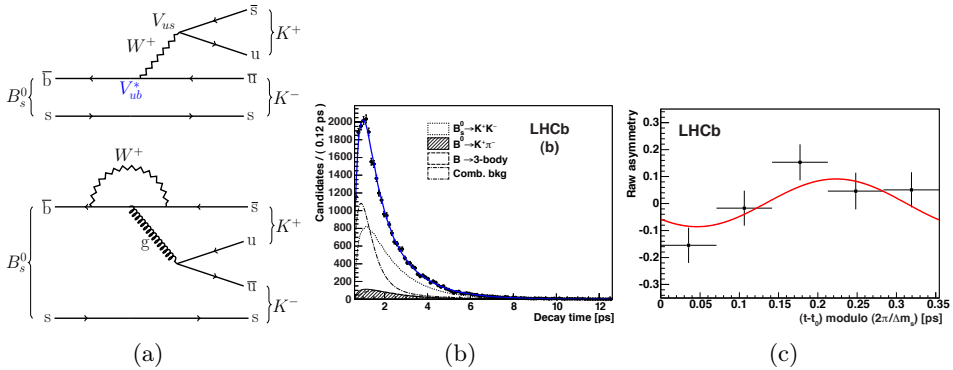


Fig. 13. (a) Feynman diagrams describing the two contributions to the decay amplitude of  $B_s^0 \rightarrow K^- K^+$ . (b) Decay time distribution and (c) time dependent CP asymmetry of  $B_s^0 \rightarrow K^- K^+$  decays. Figures (b) and (c) from Ref. [20].

In order to get a correct estimate of the observables  $S_f$  and  $C_f$ , one needs to know whether the  $B_s^0$  meson was produced as a  $B_s^0$  or a  $\bar{B}_s^0$ . At the LHC,  $B$  mesons are produced in pairs and the other  $B$  meson in the event can be used to determine the initial flavour of the signal  $B$ , by studying its decay products. In addition, a mis-tag probability is determined by means of a neural network. The method is calibrated using flavour specific  $B_s^0 \rightarrow K^- \pi^+$  decays, by exploiting the time-dependent CP asymmetry. This also yields information on the production asymmetry.

A resolution model  $R(t)$  is added to the decay equations to take into account the uncertainty on the decay time measured by LHCb. The resolution is measured on simulated  $B_s^0 \rightarrow K^- K^+$  events. Differences between data and simulated events are quantified using prompt charmonium and bottomonium data.

The acceptance describes the dependence of the reconstruction efficiency on the decay time. The acceptance function has been obtained from simulated events.

The fit to the decay time distribution of  $B_s^0 \rightarrow K^- K^+$  candidates is shown in Fig. 13 (b). The CP observables  $C_{KK}$  and  $S_{KK}$  are measured for the first time

$$\begin{aligned} C_{KK} &= 0.14 \pm 0.11 \text{ (stat.)} \pm 0.03 \text{ (syst.)}, \\ S_{KK} &= 0.30 \pm 0.12 \text{ (stat.)} \pm 0.04 \text{ (syst.)}. \end{aligned} \quad (33)$$

The values of  $(C_{KK}, S_{KK})$  differ from  $(0,0)$  with  $2.7\sigma$  significance. The largest contribution to the systematic uncertainty is from the decay time resolution model. The time dependent CP asymmetry is shown in Fig. 13 (c).

In a similar manner, the observables  $C_{\pi\pi}$  and  $S_{\pi\pi}$  are extracted from a fit to the decay time distribution of  $B^0 \rightarrow \pi^-\pi^+$  events

$$\begin{aligned} C_{\pi\pi} &= -0.38 \pm 0.15 \text{ (stat.)} \pm 0.02 \text{ (syst.)}, \\ S_{\pi\pi} &= -0.71 \pm 0.13 \text{ (stat.)} \pm 0.02 \text{ (syst.)} \end{aligned} \quad (34)$$

and are in good agreement with previous measurements.

## 6. Conclusion

We have reported on several measurements of CP violation with  $B$  meson decays carried out by the LHCb Collaboration in 2013. LHCb has produced many first and world's best CP asymmetry measurements, in many different  $B$  decay modes. Most of the current results are limited by their statistical uncertainty. All results presented here are based on the  $1 \text{ fb}^{-1}$  dataset collected in 2011. The  $2 \text{ fb}^{-1}$  dataset collected in 2012 is currently being studied and updates can be expected soon. More data is to be collected in Run 2, which is scheduled to start in 2015. The higher luminosity and center-of-mass energy available will allow LHCb to further push the era of precision flavour physics.

## REFERENCES

- [1] A. Sakharov, *Pisma Zh. Eksp. Teor. Fiz.* **5**, 32 (1967).
- [2] J. Christenson *et al.*, *Phys. Rev. Lett.* **13**, 138 (1964).
- [3] T.M.M. Kobayashi, *Prog. Theor. Phys.* **49**, 652 (1973).
- [4] L. Wolfenstein, *Phys. Rev. Lett.* **51**, 1945 (1983).
- [5] A.A. Alves Jr. *et al.* [LHCb Collaboration], *JINST* **3**, S08005 (2008).
- [6] R. Aaij *et al.* [LHCb Collaboration], *Phys. Rev. Lett.* **110**, 221601 (2013) [[arXiv:1304.6173](#) [hep-ex]].
- [7] R. Aaij *et al.* [LHCb Collaboration], *Phys. Rev. Lett.* **112**, 011801 (2014) [[arXiv:1310.4740](#) [hep-ex]].
- [8] R. Aaij *et al.* [LHCb Collaboration], *Phys. Lett.* **B726**, 151 (2013) [[arXiv:1305.2050](#) [hep-ex]].
- [9] LHCb Collaboration, LHCb-CONF-2013-006.
- [10] R. Aaij *et al.* [LHCb Collaboration], *Phys. Lett.* **B712**, 203 (2012) [[arXiv:1203.3662](#) [hep-ex]].
- [11] M. Gronau, D. Wyler, *Phys. Lett.* **B265**, 172 (1991).
- [12] M. Gronau, D. London, *Phys. Lett.* **B253**, 483 (1991).
- [13] R. Aaij *et al.* [LHCb Collaboration], *Phys. Lett.* **B723**, 44 (2013) [[arXiv:1303.4646](#) [hep-ex]].

- [14] D. Atwood, I. Dunietz, A. Soni, *Phys. Rev. Lett.* **78**, 3257 (1997) [arXiv:hep-ph/9612433].
- [15] D. Atwood, I. Dunietz, A. Soni, *Phys. Rev.* **D63**, 036005 (2001) [arXiv:hep-ph/0008090].
- [16] R. Aaij *et al.* [LHCb Collaboration], *Phys. Lett.* **B718**, 43 (2012) [arXiv:1209.5869 [hep-ex]].
- [17] A. Giri *et al.*, *Phys. Rev.* **D68**, 054018 (2003).
- [18] R. Aaij *et al.* [LHCb Collaboration], *Phys. Lett.* **B728**, 607 (2014) [arXiv:1308.1048 [hep-ex]].
- [19] R. Aaij *et al.* [LHCb Collaboration], *New J. Phys.* **15**, 053021 (2013) [arXiv:1304.4741 [hep-ex]].
- [20] R. Aaij *et al.* [LHCb Collaboration], *J. High Energy Phys.* **1310**, 183 (2013) [arXiv:1308.1428 [hep-ex]].